

ECF22 - Loading and Environmental effects on Structural Integrity

## Analysis of stress corrosion cracking in X80 pipeline steel: An approach from the theory of critical distances

P. González<sup>a\*</sup>, S. Cicero<sup>a</sup>, J.A. Álvarez<sup>a</sup>, B. Arroyo<sup>a</sup>

<sup>a</sup>LADICIM (Laboratorio de la División de Ciencia e Ingeniería de los Materiales), Universidad de Cantabria. ETS Ingenieros de Caminos, Canales y Puertos, Av/Los Castros 44, Santander 39005, España.

---

### Abstract

This paper presents an analysis of Stress Corrosion Cracking (SCC) based on the Theory of Critical Distances (TCD). The research is based on an experimental program composed of fracture specimens with notch radius varying from 0 mm (crack-like defect) up to 1 mm, and tensile specimens. A pipeline steel was used in this work (X80). It has been analysed in one hydrogen embrittlement situation. The study has been completed with Finite Elements Simulation analysis. The capacity of the TCD to analyse SCC processes has been proven.

© 2018 The Authors. Published by Elsevier B.V.

Peer-review under responsibility of the ECF22 organizers.

**Keywords:** Hydrogen Embrittlement; Theory of Critical Distances; Notch Effect; Environmental Assisted Cracking, Stress Corrosion Cracking.

---

### 1. Introduction

A critical aspect concerning high strength steels is their resistance to Stress Corrosion Cracking (SCC) and Hydrogen Embrittlement (HE) phenomena, both of which lead to degradation of the mechanical properties of these steels when facing aggressive environments (Hamilton (2011), Tiwari et al. (2000) and Rehr et al. (2014)). The effect of hydrogen is especially significant in high-strength steels exposed to aqueous environments under cathodic protection (such as off-shore platforms) or those typical of H<sub>2</sub>S presence (as in gas transport pipelines). Both phenomena, HE and SCC, are similar, resulting in brittle failures in the presence of an aggressive environment and maintained stress.

---

\* Corresponding author. Tel.: +34 622 01 47 75

E-mail address: [pablo.glez@unican.es](mailto:pablo.glez@unican.es)

## Nomenclature

### Principal symbols

$a$	crack size
$B$	specimen thickness
$B_N$	net specimen thickness
$E$	Young's modulus
$K_{IC}$	fracture toughness
$K_{IN}$	apparent fracture toughness
$K_{ISCC}^N$	apparent fracture toughness for stress corrosion cracking
$L$	material critical distance
$W$	specimen width
$\rho$	notch radius
$\sigma_U$	ultimate tensile strength
$\sigma_Y$	yield stress
$\sigma_0$	inherent strength
$\sigma_{0SCC}$	SCC threshold stress

### Principal abbreviations

FEM	Finite Elements
HE	Hydrogen Embrittlement
PM	Point Method
SCC	Stress Corrosion Cracking
TDC	Theory of Critical Distances

The defects on structural components can appear at any stage of the component's life. However, they are not always sharp. Notched components present an apparent fracture toughness which is greater than the fracture toughness observed in cracked components (Griffith (1920), Niu et al. (1998), Pluvinage (1998), Bao and Jin (1993), Fenghui (2000), Creager and Paris (1967), Cicero et al. (2008), Cicero et al. (2014)). Hence, if notches are considered as cracks when performing fracture assessments under SCC or HE conditions, the corresponding results may be overconservative, increasing the costs due to oversizing the structures, premature repairs and replacements. Thus, methodologies that consider the actual behavior of notches are necessary.

Nowadays, different researchers have developed a notch theory capable of predicting the fracture behaviour of notched components. Two main failure criteria have been proposed: the global criterion and the local criteria (Griffith (1920), Niu et al. (1998)). The local criteria are based on the stress-strain field at the notch tip and are easier to apply in practical terms. The most relevant are the Point Method (PM) and the Line Method, both of them belonging to the Theory of Critical Distances (TDC). The Theory of Critical Distances is, basically, a group of methodologies, all of which use a characteristic material length parameter, the critical distance ( $L$ ), when performing fracture assessments (Taylor (2007) Taylor et al. (2004), Neuber (1958), Peterson (1959)). The expression in fracture analysis for the above-mentioned critical distance,  $L$ , follows the equation (1):

$$L = \frac{1}{\pi} \left( \frac{K_{IC}}{\sigma_0} \right)^2 \quad (1)$$

where  $K_{IC}$  is the material fracture toughness obtained for cracked specimens and  $\sigma_0$  is a characteristic material strength parameter (the inherent strength), usually larger than the ultimate tensile strength ( $\sigma_U$ ) that requires calibration. In fatigue analysis,  $L$  has an analogous expression (Taylor (2007)). The evaluation made by the PM is particularly simple and establishes that the fracture occurs when the stress reaches the inherent strength,  $\sigma_0$ , at a distance from the defect tip equal to  $L/2$ . Consequently, the failure criterion is:

$$\sigma\left(\frac{L}{2}\right) = \sigma_0 \quad (2)$$

The TCD allows the fracture assessment of components with any kind of stress riser to be performed. As an example, when using the PM, it would be sufficient to perform two fracture tests on two specimens with different types of defects (e.g., sharp notch and blunt notch). The corresponding stress-distance curves at fracture, which can be determined by using analytical solutions or finite element methods, cross each other at a point with coordinates  $(L/2, \sigma_0)$ , as shown in Figure 1, provided both are sufficiently sharp.

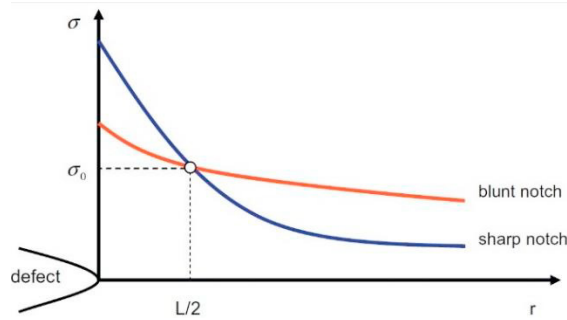


Fig. 1. Obtaining  $L$  and  $\sigma_0$  parameters.

In addition, the PM provides expressions for the apparent fracture toughness ( $K_{IN}$ ) exhibited by notched components. In the case of U-shaped notches (as those analysed in this work), the PM can be used considering a linear-elastic stress distribution at the notch tip provided by Creager and Paris (1967). The expression derived from the PM is:

$$K_{IN} = K_{IC} \frac{\left(1 + \frac{\rho}{L}\right)^{\frac{3}{2}}}{\left(1 + \frac{2\rho}{L}\right)} \quad (3)$$

Finally, the TDC is known and used to predict failure in fracture and fatigue analysis. Nevertheless, the TDC has not been applied in SCC and HE analysis. The aim of this research is, on the one hand, to study the notch effect in the apparent fracture toughness for SCC and, on the other hand, to present an SCC analysis based on the TDC.

## 2. Experimental programme

### 2.1. Material

The material employed for this study is an API X80 steel, which is widely used in oil and natural gas transportation at low temperatures due to its high strength and toughness. It has a ferritic-pearlitic microstructure shown in Figure 2. Mechanical properties of the steel, as received, are shown in Table 1.

Table 1. Mechanical properties of steels.

Parameter		X80
Yield Stress, $\sigma_y$ (MPa)		621,3
Ultimate Stress, $\sigma_U$ (MPa)		692,9
Young's Modulus, $E$ (GPa)		209,9
Ramber-Osgood Parameters	N	28,51
	$\alpha$	0,64

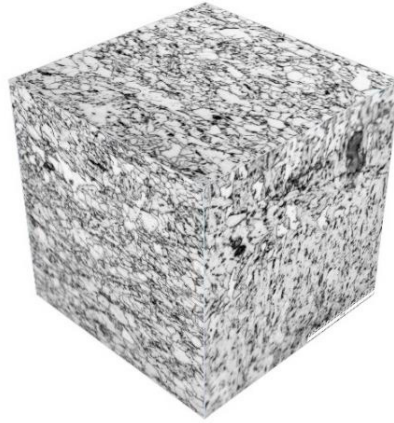


Fig. 2. X80 microstructure.

## 2.2. Simulation of Hydrogen Embrittlement

Cathodic charge has been employed in this study. It is used to protect against corrosion components that operate in aggressive environments or to reproduce local situations where a high amount of hydrogen is present. The disadvantage is that it causes embrittlement on the steel by the action of the hydrogen going through and getting trapped in it. Figure 3 presents a set-up of the method used in this work. The steel is connected, through an acid electrolyte, with a noble metal (platinum). The steel will be protected because of a fixed current interposed. The acid electrolyte, in accordance with the literature (Arroyo et al. (2017), Pressouyre (1977)), consists of an 1N H<sub>2</sub>SO<sub>4</sub> solution in distilled water with 10 drops of CS<sub>2</sub> and 10mg of an As<sub>2</sub>O<sub>3</sub> solution (prepared using Pressouyre's method) dissolved per liter of dissolution.

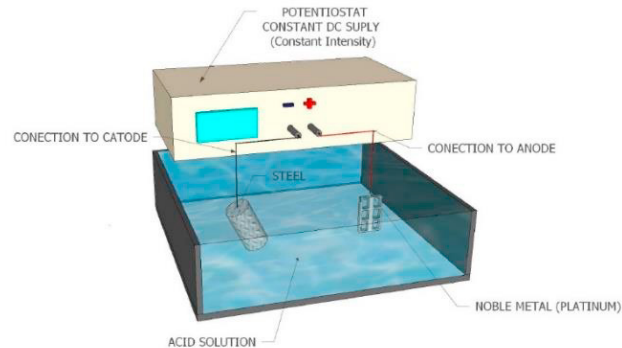


Fig. 3. Schematic of the cathodic charge method.

This work has used a cathodic polarization with a current interposed at a level of 5 mA/cm<sup>2</sup>. This setup is widely used in order to protect gas and petroleum pipes and offshore structures (Siddiqui (2005))

## 2.3. Experimental programme

Following the expressions given by the TDC in fracture and fatigue analysis, the following expressions have been proposed for SCC analysis:

$$L = \frac{1}{\pi} \left( \frac{K_{ISCC}}{\sigma_{SCC}} \right)^2 \quad (4)$$

$$K_{ISCC}^N = K_{ISCC} \frac{\left(1 + \frac{\rho}{L}\right)^{\frac{3}{2}}}{\left(1 + \frac{2\rho}{L}\right)} \quad (5)$$

In order to analyse the suitability and accuracy of these expressions, it is necessary to perform a set of tests. Firstly, fracture mechanics tests were carried out in order to determine  $K_{ISCC}$  in the environmental condition described (cathodic charge at 5 mA/cm<sup>2</sup>). Before the test, pre-cracked CT specimens were exposed to hydrogen absorption for 48h at the same environmental and aggressiveness conditions. The tests were performed using a slow strain rate machine. Following the recommendations of the Standard ISO-7539, the tests were performed at 6·10<sup>-8</sup> m/s of constant solicitation rate. The TDC parameters have been calibrated with fracture tests on CT notched specimens. The notched samples were tested under the same conditions as the previous test.

Secondly, tensile tests were carried out as per an accelerated method to measure the threshold stress ( $\sigma_{SCC}$ ) defined in ASTM F1624. This test method establishes a procedure to measure the susceptibility of steel to a time-delayed failure (such as that caused by hydrogen) based on incremental step load. This test requires that a minimum of three samples to be tested in order to establish the threshold load, which is calculated from the load at the last step to maintain the load for the duration of the step. Figure 4 shows the geometry of the CT notched specimen (a) and the tensile specimen (b).

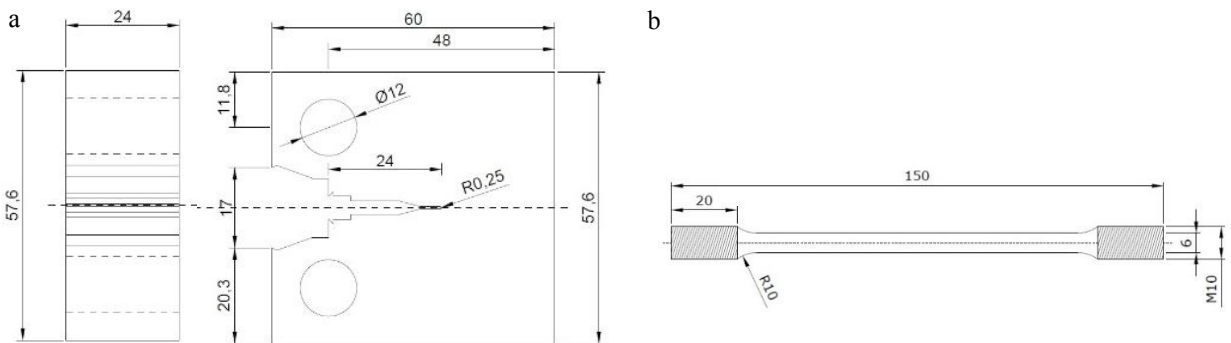


Fig. 4. (a) Schematic showing the geometry of the CT notched specimens,  $\rho$  varying from 0 mm to 1.0 mm (in the picture  $\rho=0.25$ mm); (b) Tensile specimens. Dimensions in mm.

### 3. Finite Elements Simulations

Finite Elements (FE) modelling was performed (ABAQUS 6.13) in order to determine the defect tip stress field at failure in the different specimens. Each geometry, corresponding to one of the sets, was conducted to the average failure load of the different tests composing the set. The stress–distance curve in the middle line of the section was obtained (starting from the defect tip). The stress obtained was the maximum principal stress. According to Taylor (2007), Taylor et al. (2004), the simulation was conducted in linear-elastic conditions. Also, the mesh was performed using hexahedric elements, the mesh being much more refined at the defect tip, because of the higher gradients appearing in this zone, Fig. 5.

When applying the TCD through the PM to multiple geometries, other works (e.g., Taylor (2007), Taylor et al. (2004)) generally present just two curves to show how simple this methodology can be. Assuming this simplicity, all the curves are represented with the aim of guiding the reader in the interpretation of the results and to clarify some precautions that should be kept in mind when applying the TCD.

The different curves cross each other at one point, so the application of the PM, and then the whole TCD, could be possible. This point will serve to obtain the material critical distance,  $L$ .

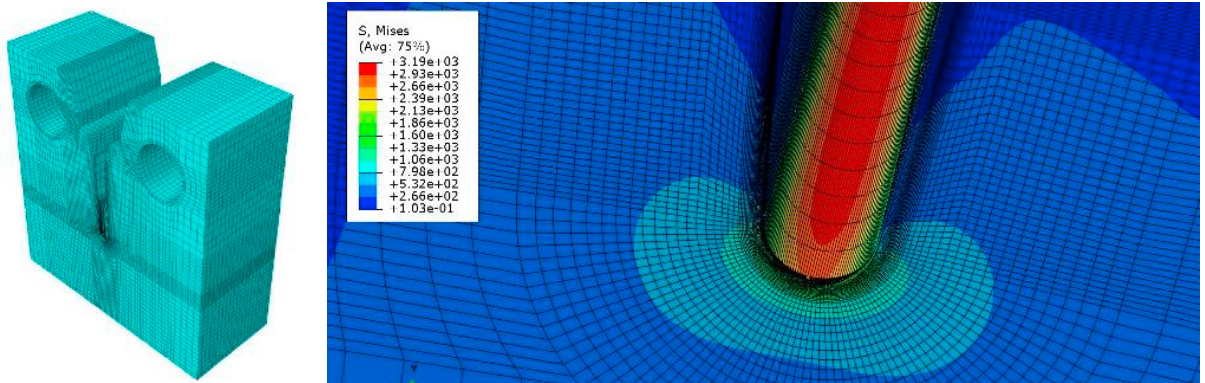


Fig. 5. Mesh of the CT specimen and Von-Mises stress distribution around the U-notch.

#### 4. Results and discussion

The methodology proposed by ASTM E-1820 was employed for the  $K_{ISCC}$  value calculation (see Eq. 6). Table 2 gathers the experimental results obtained and **figure 6** shows one of the tests during its performance.

$$K_{ISCC}^N = \frac{P_Q}{(BB_N W)^{1/2}} \frac{[(2 + a/W)(0.886 + 4.64(a/W) - 13.32(a/W)^2 + 14.72(a/W)^3 - 5.6(a/W)^4)]}{(1 - a/W)^{3/2}} \quad (6)$$

where  $P_Q$  is the load at the moment of crack initiation,  $B$  is the specimen thickness,  $W$  is the specimen width and  $a$  is the defect length.

Table 2. Experimental results.

Notch radius, $\rho$ (mm)	Notch length (mm)	Max. load (kN)	$K_{ISCC}^N$ (MPa·m <sup>0.5</sup> )
0,00	28,3	31,58	67,42
0,00	27,5	24,24	53,16
0,25	24	37,72	58,73
0,50	24	40,48	70,28
1,00	24	47,96	83,10

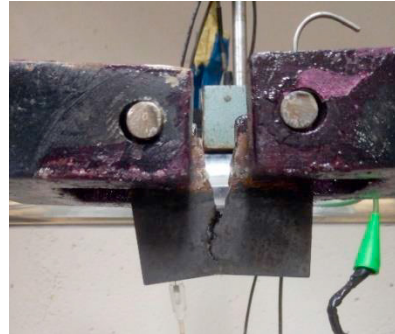
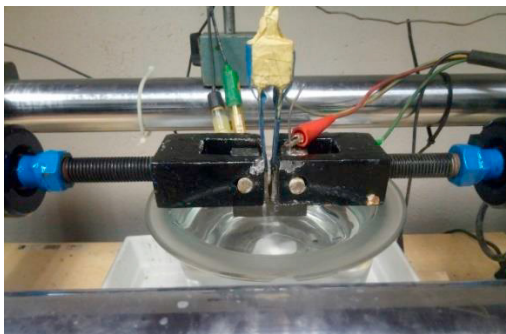


Fig. 6. Fracture mechanics test. Test during mechanical solicitation.

Figure 7 shows the incremental step loading technique, defined by ASTM F-1624 and gathers the three tensile tests. The value of  $\sigma_{SCC}$ , under the environmental conditions defined previously, is 549 MPa.



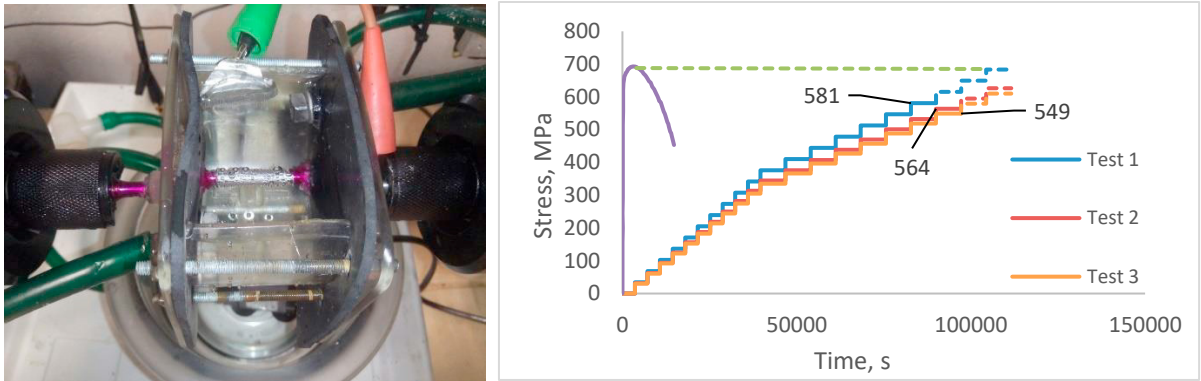


Fig. 7. Incremental Step Loading Technique and stress-time curves obtained.

From the results obtained by the finite elements analysis, the following considerations can be made:

- Figure 8 shows that the corresponding stress-distance curves cross each other at a point with coordinates  $(L/2, \sigma_0)$
- The value of  $L$  calculated from the finite elements analysis ( $L/2=0.072\text{mm}$ ) provides adjusted predictions of  $K_{ISCC}^N$  (see Fig 9) following the PM expression (Eq. 5).
- The value of  $\sigma_0$  obtained (2710 MPa) does not coincide with  $\sigma_{SCC}$  calculated (549 MPa).

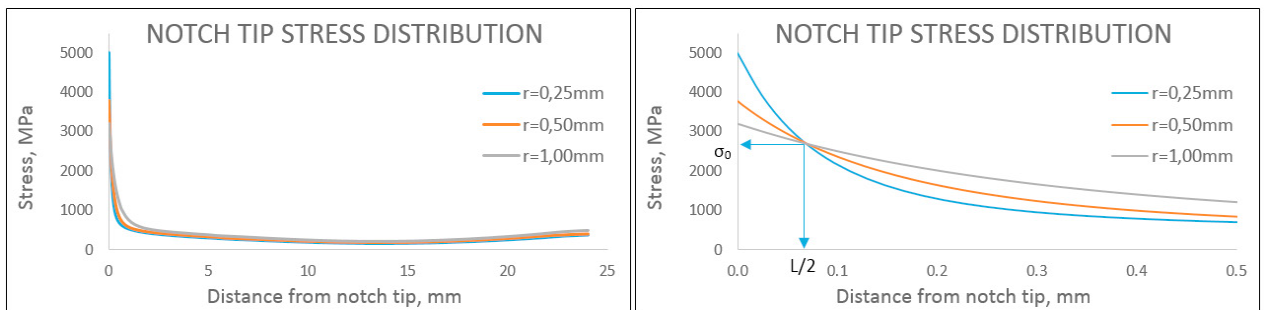


Fig. 8. Stress-distance curves at rupture in X80 CT specimens.

Figure 9 shows the experimental results of  $K_{ISCC}$  (pre-cracked specimens),  $K_{ISCC}^N$  (notched specimens) and predictions provided by the PM (Eq. 5). It can be observed that PM predictions show a high degree of accuracy.

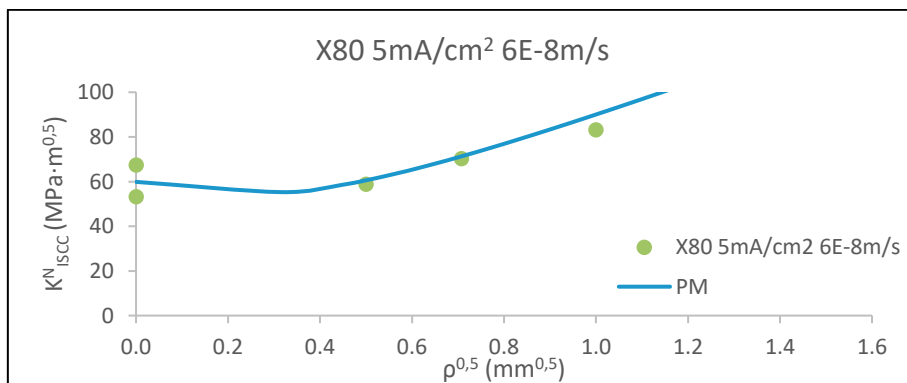


Fig. 9. Experimental results on X80 at  $5\text{mA}/\text{cm}^2$  and  $6\text{E}-8\text{m}/\text{s}$  test rate and predictions provided by the Point Method.

#### 4. Conclusions

This paper applies the Theory of Critical Distances in X80 pipeline steel to the analysis of Stress Corrosion Cracking and Hydrogen Embrittlement phenomena. The calibration of the TCD parameter can be performed by a combination of the experimental programme and FE simulations. The obtained value of  $\sigma_0$  does not coincide with  $\sigma_{SCC}$ . For that reason, it has to be calibrated with more tests in order to establish any relationship between the  $\sigma_0$  obtained and the  $\sigma_{SCC}$  calculated. An evident notch effect has been observed, with an increase in the SCC resistance in notched conditions when the notch radius increases. This effect has been predicted by the direct application of the Point Method proving the capacity of the TCD to analyse SCC processes.

#### Acknowledgements

The authors of this paper would like to thank the Spanish Ministry of Economy and Competitiveness for the support received for the research project MAT2014-58738-C3-3-R developed by the University of Cantabria.

#### References

- Álvarez, J.A., 1998. Fisuración inducida por hidrógeno de aceros soldables microaleados. Caracterización y modelo de comportamiento, Doctoral Thesis, University of Cantabria.
- Arroyo, B., Álvarez, J.A., Lacalle, R., Uribe, C., García, T.E., Rodríguez, C., 2017. Analysis of key factors of hydrogen environmental assisted cracking evaluation by small punch test on medium and high strength steels. *Materials Science and Engineering A* 691, 180-194.
- ASTM E1820 - Standard Test Method for Measurement of Fracture Toughness.
- ASTM F1624 - Standard Test Method for Measurement of Hydrogen Embrittlement Threshold in Steel by the Incremental Step Loading Technique.
- Bao, Y., Jin, Z., 1993. Size effects and mean strength criterion for ceramics. *Fatigue & Fracture of Engineering Materials & Structures* 16, 829-835.
- Cicero, S., Gutiérrez-Solana, F., Álvarez, J.A., 2008. Structural Integrity assessment of components subjected to low constraint conditions. *Engineering Fracture Mechanics* 75, 3038-3059.
- Cicero, S., Madrazo, V., Carrascal, I.A., 2012. On the point method and the line method notch effect predictions in Al7075-T651. *Engineering Fracture Mechanics* 86, 56-72.
- Cicero, S., Madrazo, V., García, T., 2014. Analysis of the notch effect in the apparent fracture toughness and the fracture micromechanisms of ferritic-pearlitic steels operating within their lower shelf. *Engineering Failure Analysis* 36, 322-342.
- Creager, M., Paris, C., 1967. Elastic field equations for blunt cracks with reference to stress corrosion cracking. *International Journal of Fracture Mechanics* 3, 247-252.
- Fenghui, W., 2000. Prediction of intrinsic fracture toughness for brittle materials from the apparent toughness of notch-crack specimen. *Journal of Materials Science* 35, 2543-2546.
- Griffith, A.A., 1920. The phenomena of rupture and flow in solids. *Phil. Trans. R Soc. London. A* 221, 163-198.
- Hamilton, J.M., 2011. The challenges of Deep-Water Arctic Development, *International Journal of Offshore and Polar Engineering* 21, 241-247.
- ISO-7539 - Corrosión de metales y aleaciones. Ensayos de corrosión bajo tensión.
- Neuber, H., 1958. *Theory of notch stresses: principles for exact calculation of strength with reference to structural form and material*. Springer Verlag, Berlin.
- Niu, L.S., Chehimi, C., Pluvinau, G., 1998. Stress field near a large blunted V notch and application of the concept of notch stress intensity factor to the fracture of very brittle materials. *Engineering Fracture Mechanics* 49, 325-335.
- Peterson, R.E., 1959. Notch sensitivity. In: Sines G, Waisman JL, editors. *Metal fatigue*. McGraw Hill, 293-306. New York.
- Pluvinau, G., 1998. Fatigue and fracture emanating from notch; the use of the notch stress intensity factor. *Nuclear Engineering and Design* 185, 173-184.
- Pressouyre, G.M., Bernstein, I.M., 1977. The role of trapping on hydrogen transport and embrittlement. Carnegie Mellon University Pittsburgh Pa Department of Metallurgy and Materials Science.
- Rehrl, J., Mraczek, K., Pichler, A., Werner, E., 2014. Mechanical properties and fracture behavior of hydrogen charged AHSS/UHSS grades at high- and low strain rate tests. *Materials Science & Engineering A* 590, 360-367.
- Siddiqui, R.A., Abdullah, H.A., 2005. Hydrogen embrittlement in 0.3% carbon steel used for petrochemical applications. *Journal of materials processing technology* 170, 430-435.
- Taylor, D., Merlo, M., Pegley, R., Cavatorta, M.P., 2004. The effect of stress concentrations on the fracture strength of polymethylmethacrylate. *Materials Science and Engineering A* 382, 288-294.
- Taylor, D., 2007. *The theory of critical distances: a new perspective in fracture mechanics*, Elsevier.
- Tiwari, G.P., Bose, A., Chakravarty, J.K., Wadekar, S.L., Totlani, M.K., Arya, R.N., Fotedar, R.K., 2000. A study of internal hydrogen embrittlement of steels. *Materials Science and Engineering A* 286, 269-281.